

Circuit optimization for IBM processors: A way to get higher fidelity and higher values of nonclassicality witnesses

Mitali Sisodia¹, Abhishek Shukla², Alexandre A. A. de Almeida³,
Gerhard W. Dueck⁴, Anirban Pathak¹

January 1, 2019

¹Jaypee Institute of Information Technology, A 10, Sector 62, Noida, UP 201307

²University of Science and Technology of China, Hefei 230026, P. R. China

³Department of Electrical Engineering, FEIS - Univ Estadual Paulista, Ilha Solteira, Brazil

⁴Faculty of Computer Science, University of New Brunswick, Canada

Abstract

Recently, various quantum computing and communication tasks have been implemented using IBM's superconductivity-based quantum computers which are available on the cloud. Here, we show that the circuits used in most of those works were not optimized and the use of the optimized circuits can considerably improve the possibility of observing unique features of quantum mechanics. Specifically, a systematic procedure is used here to obtain optimized circuits (circuits having reduced gate count and number of levels) for a large number of Clifford+T circuits which have already been implemented in the IBM quantum computers. Optimized circuits implementable in IBM quantum computers are also obtained for a set of reversible benchmark circuits. With a clear example, it is shown that the reduction in circuit costs enhances the fidelity of the output state (with respect to the theoretically expected state in the absence of noise) as lesser number of gates and levels introduce lesser amount of errors during evolution of the state. Further, considering Mermin inequality as an example, it's shown that the violation of classical limit is enhanced when we use an optimized circuit. Thus, the approach adopted here can be used to identify relatively weaker signature of quantumness and also to establish quantum supremacy in a stronger manner.

1 Introduction

Since its introduction quantum computing has drawn considerable attention of the scientific community because of the fact that it can perform certain computational tasks much faster than its classical counterparts [1, 2]. For example, it can search an unsorted database [1], solve the discrete logarithm and prime factorization problems in a speed not achievable by its classical counterparts [2]. Similarly, quantum communication has also drawn considerable attention, as it can perform classically impossible tasks like teleportation [3] and as it can provide unconditional security—an extremely desired feature that's not achievable in the classical world (see [4] and references therein). These facts led to several theoretical proposals for quantum computation and communication. Some of them have also been verified experimentally. However, the access to experimental facilities were restricted until the recent past and it was not available to most of the researchers. The scenario has been changed considerably with the introduction of a set of quantum computers by the IBM corporation [5]. These quantum computers are placed in the cloud and researchers can access them for free. Naturally, quantum computing research received a boost with it, and several computational tasks (e.g., Bell state discrimination [6], teleportation using optimal quantum resources [7], quantum permutation algorithm [8], creation of a quantum check [9], testing Mermin inequalities [10]) have recently been realized using IBM quantum computers. In these works, circuits formed using Clifford+T gates

have been used as IBM quantum computers allow only these gates. However, no serious effort has yet been made to optimize the circuits. Although the need for optimization was clear from the observations of various works [6], where it was clearly observed that the increase in gate count reduces the fidelity of the output state. In fact, there exists a direct (although not linear) correlation between the gate count and the fidelity of the experimentally obtained output state and the output state that would have been in the absence of noise. Further, quantum process tomography of the gates used in IBM quantum computers has been performed by some of the present authors [11], and the same has revealed that the gate fidelity of the gates used in IBM quantum computers are usually lower than the same obtained in other technologies, like NMR. Because of these facts, any particular architecture of IBM quantum computers imposes an upper-bound on the number of gates that can be used to construct an experimentally realizable quantum circuit with a reliable output. These limitations of the IBM quantum computers lead to the requirement that to obtain the best possible results using the IBM quantum computers, the number of gates in circuits should be minimized. Keeping this requirement in mind, in a recent work, some of the present authors designed an algorithm that can provide optimized Clifford+T circuits [12]. The same algorithm is used here to obtain optimized circuits corresponding to a set of interesting Clifford+T circuits that have been implemented using IBM quantum computers. In addition, a large number of reversible circuits are converted to Clifford+T circuits and optimized to show the usefulness of the approach used here and to establish that those circuits can also be implemented reliably using IBM quantum computers. Further, in what follows in the context of Mermin inequalities, it is shown that the optimized circuits not only provide better fidelity it also enhances the amount by which the classical limit is violated. In other words, an optimized quantum circuit can more clearly reveal the nonclassical features, and thus help to strongly establish quantum supremacy. The beauty of the approach adopted here is that the method used is very general in nature and the optimization algorithm can be easily transformed from one architecture to another architecture of quantum computer.

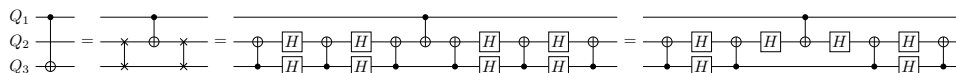
The rest of the paper is structured as follows. Section 2 briefly describes the method adopted here for obtaining the optimized quantum circuits. In Section 3, we establish the benefits (advantages) of optimization through an illustrative example. In Section 4, the work of previous section is extended to provide optimized circuits for various quantum computing tasks. However, the improvement is quantified only through the number of levels and gate count. Further, a large set of reversible circuits are also optimized. Finally, the paper is concluded in Section 5.

2 Optimized Clifford+T quantum circuits for IBM's QX2 and QX4 architectures

IBM has made several quantum computers available via cloud services. Among them are two 5-qubit quantum computers (QX2 and QX4) [5] whose architectures are shown in Fig. 1. The arrows between the qubits indicate the CNOT gates that are allowed to be implemented directly in a particular architecture. Specifically, the head of an arrow indicates the target qubit and the other side corresponds to a control qubit. Thus, IBM quantum computers do not allow us to directly implement all the CNOT gates. However, all single qubit gates from the Clifford+T gate library can be implemented directly. Consequently, an arbitrary Clifford+T circuit may not be implementable directly in an IBM quantum processor. A CNOT gate that is not supported by the architecture can be realized with a sequence of gates (for details see [12]).

The Basic idea in [12] is to find a realization for every possible CNOT operation in a given architecture. This can be accomplished by swapping qubits until they are connected by a CNOT. Next, the CNOT is applied and finally the qubits are swapped back to their original place. There are many sequence of swaps that can accomplish the same objective. For each transformation, there are also some reduction in the number of gates. For example, to realized $\text{CNOT}(Q_1, Q_4)$ on QX2, the qubits Q_2 and Q_4 can be swapped, followed by $\text{CNOT}(Q_2, Q_4)$, and finally Q_2 and Q_4 are swapped again. The SWAPs can be realized with a cost of 10 additional gates, after some reduction as shown below.

An alternative transformation with one fewer gate can be achieved as follows [12].



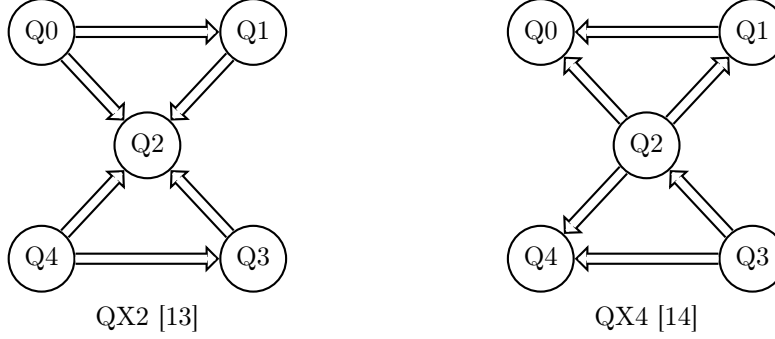
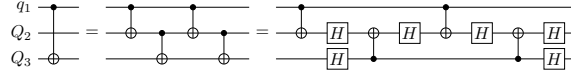


Figure 1: Architectures of IBM's five-qubit processors.



The algorithmic approach adopted here requires that all such transformations, with their corresponding cost (number of additional gates) are to be stored in a table. This table has to be build only once for every architecture. It will take one table look up to find the best realization for $\text{CNOT}(a, b)$. All CNOT gates in a given circuit Clifford+T circuits are to be replaced with their equivalent transformations.

It is clear that different mappings of logical qubits to the physical ones will yield different costs in the target architecture. For example, if a circuit contains the following gates $\text{CNOT}(a, b)$ and $\text{CNOT}(b, c)$. An optimal mapping for QX2 would be $\{a \rightarrow Q0, b \rightarrow Q1, c \rightarrow Q2\}$ whereas for QX4 it would be $\{a \rightarrow Q3, b \rightarrow Q2, c \rightarrow Q0\}$. Thus, the optimized circuit to be obtained would depend on the architecture of the quantum processor, but the method to be followed is independent of the architecture.

For a circuit with only five qubits, it is feasible to calculate the cost for all 120 permutations and pick the best one. this is exactly what is proposed in [12]. Finally, some simplifications may be possible. For example, the transformation may yield two consecutive Hadamard gates on the same qubits, which can be removed. Other more complex circuit identities or templates can also be used.

3 Benefit of the optimization: An illustrative examples

We have already mentioned that various quantum computing tasks have been performed using IBM's QX2 and QX4, but the corresponding circuits were not optimized. In this section, we select some of those circuits to establish that the optimized circuit can yield better results and reveal quantumness in a stronger manner. Specifically, we have chosen a set of circuits implemented in QX2 to demonstrate experimental violation of Mermin inequalities. These circuits are of particular importance for various reasons, especially for the fact that Mermin inequalities being an extension of Bell's inequalities to the multi-partite scenario can be used to discriminate between classical physics and quantum physics, and establish the nonlocal nature of the physical world. In other words, an experimentally observed violation of a Mermin inequality can strongly establish that the physical world cannot be described by local hidden variable theories. This is somewhat obvious as Mermin inequities are essentially Bell type inequalities. Violation of Bell's inequality has been shown in many experiments, but it's slightly more difficult to show the violation of Mermin inequality as it's difficult to achieve a good control of three or more qubits, including the generation of entangled states (say a GHZ-type state which maximally violates Mermin inequality) [10]. This is where an optimized circuit may play a crucial role by providing greater control and higher fidelity.

3.1 Circuits for the realization of Mermin inequality

Violation of any of the Mermin inequalities implies the existence of a situation that cannot be explained classically. In the recent past, violation of Mermin inequality has been shown using various techniques, including ion-trap [15], and optics-based [16] techniques. One of the most recent experiment in this line has

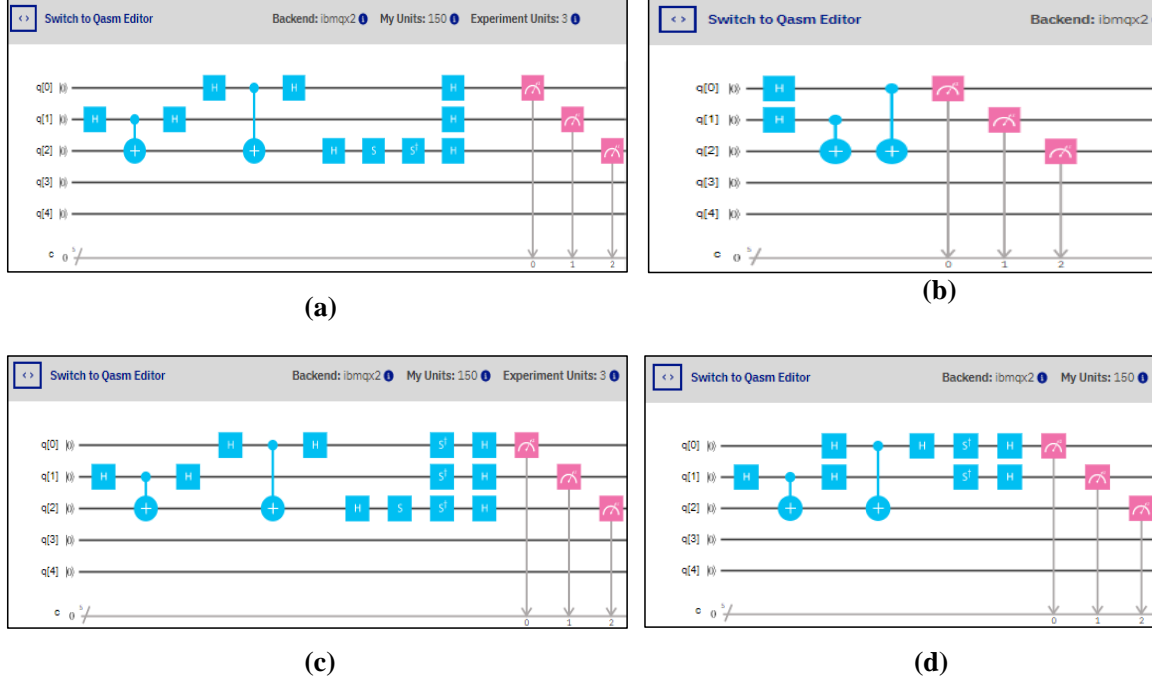


Figure 2: (Color online) (a) and (c) show the circuits used in Fig. 1 of [10] to demonstrate violation of Mermin inequality in tripartite scenario. Optimized equivalent circuits for (a) and (c) are shown as (b) and (d), respectively.

been done by Alsina and Latorre in 2016 [10]. They have demonstrated violation of Mermin inequalities using IBM's QX2 quantum computing processor. The work was done almost immediately after the access to QX2 was provided. In their work, they had shown violation of Mermin inequalities for $n = 3$ to $n = 5$. For $n = 3$ case, i.e., in a tripartite scenario, they used the circuits shown in Fig. 2 (a) and (c) (cf. Fig. 1 of [10]). We have used our algorithm to optimize these circuits. The optimized circuits corresponding to the circuits shown in Fig. 2 (a) and (c) are shown in Fig. 2 (b) and (d), respectively. It is clearly visible that the optimized circuits have smaller gate counts and levels. Specifically the circuit shown in Fig. 2 (a) has 12 gates and 7 levels, but the corresponding optimized circuit (shown in Fig. 2 (b)) has only 4 gates and 3 levels. Thus, the gate count has been reduced by 67% and the number of levels have been reduced by 57%. Similarly, for the circuit shown in Fig. 2 (c) has 14 gates and 8 levels, but the corresponding optimized circuit (as shown in Fig. 2 (d)) has only 10 gates and 6 levels. Thus, the optimization scheme adopted here can considerably reduce the circuit costs and provide efficient circuits. However, reduction in circuit costs is not the only parameter that can quantitatively illustrate the necessity and advantages of the optimization procedure. There are other ways to check whether the optimization process has improved the performance of the circuit.

To begin with we run the circuits shown in Fig. 2 for 8,192 times each by using QX2 processor. Originally, in [10], the unoptimized circuits were run for 1,024 times. The output of our experiment is specifically shown in Fig. 3, where the left panel corresponds to the output of the circuit shown in Fig. 2 (a) whereas the right panel illustrates the experimental output of the corresponding optimized circuit. These outputs are just representative. The complete set of similar results obtained by realizing the circuits shown in Fig. 2 using QX2 is given in Table 1. This table can be used to compute violation of Mermin inequality in each case. Here, we may note that for $n = 3$, i.e., for 3-qubit case, the expectation value of the Mermin polynomial for a classical theory (which essentially obeys local realism) is bounded by 2 (i.e., $\langle M_3 \rangle_{\text{classical}} \leq 2$), whereas for quantum mechanics (QM) it is bounded by 4 (i.e., $\langle M_3 \rangle^{\text{QM}} \leq 4$). Now, we may consider $\langle M_3 \rangle - 2$ as a measure of how strongly Mermin inequality is violated by a 3-qubit state. In fact, we can calculate $\langle M_3 \rangle$ using Table 1, by following the method used in [10]. This method uses the formula $\langle M_3 \rangle = 3\langle XXY \rangle - \langle YYY \rangle$ where $\langle A \rangle = \sum_i P_i E_i$, with P_i is the probability of system being found in the i^{th} eigenstate of operator

Circuit	No. experiments	P_{000}	P_{001}	P_{010}	P_{011}	P_{100}	P_{101}	P_{110}	P_{111}
Fig. 2 a	1,024	0.229	0.042	0.024	0.194	0.043	0.203	0.231	0.033
Fig. 2 a	8,192	0.238	0.041	0.035	0.202	0.031	0.223	0.217	0.013
Fig. 2 b	8,192	0.239	0.031	0.027	0.224	0.029	0.224	0.214	0.012
Fig. 2 c	1,024	0.050	0.188	0.188	0.028	0.258	0.026	0.041	0.221
Fig. 2 c	8,192	0.046	0.223	0.210	0.033	0.218	0.029	0.028	0.214
Fig. 2 d	8,192	0.048	0.219	0.215	0.037	0.216	0.023	0.032	0.210

Table 1: Results of Mermin experiment are provided in the table. P_i show the probability of finding the state $|i\rangle$ on measuring the output state in the computational basis. Results of the circuit given in the Fig. 2 a are shown in the first row for 1024 runs and for 8192 runs in the second row. Results of the circuit given in Fig. 2 b are provided in the second row for 8192 runs. Similarly, results of the Fig. 2 c are given in the rows third and fourth for 1024 and 8192 runs, respectively. Ultimately, results of the circuit in the Fig. 2 d are given in last row.

No. of qubits	[10]'s circuits (1024 runs)	[10]'s circuits (8192 runs)	Optimized circuits (8192 runs)
3 qubits	2.85 ± 0.02	3.009	3.126

Table 2: A comparison of the value of $\langle M_3 \rangle$ obtained originally in [10], where the experiment was run for 1024 times with that obtained by running the same experiment for 8192 times and running the optimized circuit for 8192 times.

A and E_i is the eigenvalue of the corresponding state. The experimental setup for the measurement of $\langle XXY \rangle \langle YYY \rangle$ is given in Figs. 2 a and c (Figs. 2 b and d). Thus, using P_i s given in Table 1 we can compute $\langle M_3 \rangle$ which is 3.126 in our case in contrast to the value of 2.85 ± 0.02 obtained in the original work of Alsina and Latorre [10]. As we have already mentioned that $\langle M_3 \rangle > 2$ implies the violation of Mermin inequality or the nonexistence of a classical local realistic (LR) theory, our result establishes the existence of a nonclassical theory in general (quantum mechanics in particular). The observed value of 3.126 (> 2.85) for optimized case indicates that the optimized circuits can witness the signature of nonclassicality in a stronger manner. Thus, in those cases where Mermin inequalities or other similar inequalities are violated weakly, optimized circuits will be of much relevance in identifying the signature of nonclassicality.

Even this set of experiments does not give the whole picture. To further illustrate the benefit of the circuit optimization procedure adopted here, we need to perform quantum state tomography (QST). In order to perform QST using IBM quantum processors, one can adopt the procedure described in our earlier works (see [6]) which will require some additional experiments. Here, we restrict ourselves from describing the procedure adopted for performing QST and directly report the relevant density matrices.

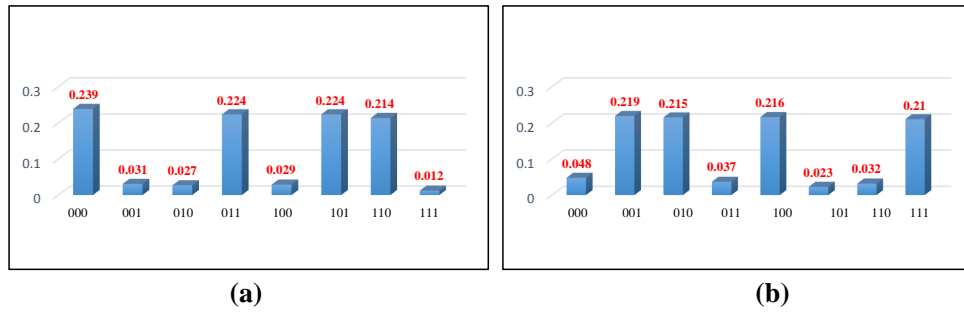


Figure 3: (Color online) ((a) and (b)) represent the obtained probability distribution for circuits shown in Figs. 2 (a) and (b), respectively.

Ideal density matrix corresponding to the output state of the circuit shown in Fig. 2 (a) is

$$\rho_{ideal} = \begin{pmatrix} \frac{1}{4} & 0 & 0 & \frac{1}{4} & 0 & \frac{1}{4} & \frac{1}{4} & 0 \\ 0 & 0 & 0 & 0 & 0 & 0 & 0 & 0 \\ 0 & 0 & 0 & 0 & 0 & 0 & 0 & 0 \\ \frac{1}{4} & 0 & 0 & \frac{1}{4} & 0 & \frac{1}{4} & \frac{1}{4} & 0 \\ 0 & 0 & 0 & 0 & 0 & 0 & 0 & 0 \\ \frac{1}{4} & 0 & 0 & \frac{1}{4} & 0 & \frac{1}{4} & \frac{1}{4} & 0 \\ \frac{1}{4} & 0 & 0 & \frac{1}{4} & 0 & \frac{1}{4} & \frac{1}{4} & 0 \\ 0 & 0 & 0 & 0 & 0 & 0 & 0 & 0 \end{pmatrix}. \quad (1)$$

Density matrix of the actual state generated in the experimental realization of the circuit shown in Fig. 2 (a) is obtained by QST, and the real and imaginary parts of that density matrix is given below

$$Re[\rho_{ex}A] = \begin{pmatrix} 0.238 & 0.03 & 0.007 & 0.098 & 0.005 & 0.115 & 0.095 & -0.016 \\ 0.03 & 0.031 & 0.094 & 0.019 & 0.118 & 0.002 & 0.012 & 0.094 \\ 0.007 & 0.094 & 0.035 & -0.002 & 0.091 & -0.009 & 0.001 & 0.097 \\ 0.098 & 0.019 & -0.002 & 0.217 & 0.017 & 0.093 & 0.097 & 0.002 \\ 0.005 & 0.118 & 0.091 & 0.017 & 0.041 & 0.030 & 0.034 & 0.095 \\ 0.115 & 0.002 & -0.009 & 0.093 & 0.030 & 0.223 & 0.094 & -0.02 \\ 0.095 & 0.012 & 0.001 & 0.097 & 0.034 & 0.094 & 0.202 & -0.016 \\ -0.016 & 0.094 & 0.097 & 0.002 & 0.095 & -0.02 & -0.016 & 0.013 \end{pmatrix}, \quad (2)$$

and

$$Im[\rho_{ex}A] = \begin{pmatrix} 0 & 0.005 & 0.002 & -0.065 & -0.002 & -0.01 & -0.029 & -0.005 \\ -0.005 & 0 & -0.001 & -0.0045 & 0.009 & -0.002 & -0.003 & -0.019 \\ -0.002 & 0.001 & 0 & -0.012 & 0.034 & -0.0015 & 0.002 & 0.001 \\ 0.065 & 0.004 & 0.012 & 0 & 0.009 & 0.021 & 0.002 & 0 \\ 0.002 & -0.009 & -0.034 & -0.009 & 0 & -0.006 & 0.002 & -0.0002 \\ 0.01 & 0.002 & 0.001 & -0.021 & 0.006 & 0.223 & -0.049 & -0.006 \\ 0.029 & 0.003 & -0.002 & -0.002 & -0.002 & 0.049 & 0 & 0.006 \\ 0.0052 & 0.019 & -0.001 & 0 & 0.0002 & 0.006 & -0.006 & 0 \end{pmatrix}, \quad (3)$$

Similarly, real and imaginary parts of experimental density matrix of the output state of the corresponding optimized circuit shown in Fig. 2 (b) can be obtained by QST as

$$Re[\rho_{ex}B] = \begin{pmatrix} 0.239 & 0.032 & -0.004 & 0.199 & 0.032 & 0.21 & 0.183 & -0.014 \\ 0.032 & 0.029 & 0.005 & 0.021 & 0.023 & 0.023 & 0.019 & 0.007 \\ -0.004 & 0.005 & 0.027 & -0.0125 & 0.004 & -0.003 & -0.009 & 0.010 \\ 0.199 & 0.021 & -0.012 & 0.214 & 0.035 & 0.182 & 0.197 & -0.016 \\ 0.032 & 0.023 & 0.004 & 0.035 & 0.031 & 0.031 & 0.030 & -0.001 \\ 0.21 & 0.023 & -0.003 & 0.182 & 0.031 & 0.224 & 0.184 & -0.019 \\ 0.18 & 0.019 & -0.009 & 0.197 & 0.030 & 0.184 & 0.224 & -0.019 \\ -0.014 & 0.007 & 0.010 & -0.0165 & -0.001 & -0.019 & -0.019 & 0.012 \end{pmatrix} \quad (4)$$

and

$$Im[\rho_{ex}B] = \begin{pmatrix} 0 & -0.009 & 0.004 & -0.050 & -0.010 & 0.002 & -0.064 & -0.010 \\ 0.009 & 0 & 0.0002 & -0.008 & 0.001 & -4.3 \times 10^{-19} & -0.007 & -0.019 \\ -0.004 & -0.0002 & 0 & -0.014 & -0.010 & -0.008 & -0.016 & 0.005 \\ 0.050 & 0.008 & 0.014 & 0 & 0.008 & 0.032 & -0.008 & -0.007 \\ 0.01 & -0.001 & 0.010 & -0.0081 & 0 & -0.001 & -0.005 & 0.002 \\ -0.002 & 4.3 \times 10^{-19} & 0.008 & -0.032 & 0.001 & 0 & -0.050 & -0.004 \\ 0.064 & 0.007 & 0.016 & 0.008 & 0.005 & 0.050 & 0 & -0.009 \\ 0.01 & 0.019 & -0.005 & 0.007 & -0.002 & 0.004 & 0.0095 & 0 \end{pmatrix}. \quad (5)$$

To establish the relevance of the present study, i.e., optimization of quantum circuits, we have used a distance based measure to quantify the performance of a quantum circuit known as fidelity, which is defined as $F = \text{Tr}[\sqrt{\sqrt{\rho_1} \cdot \rho_2 \cdot \sqrt{\rho_1}}]$, where ρ_1 and ρ_2 correspond to two quantum states to be compared. Specifically, we have computed the fidelity between the quantum state expected in the ideal scenario (ρ_{ideal} in Eq. (1)) with that obtained in the real experiments using QX2 ($\rho_{ex}A$ in Eq. (2) and in Eq. (3)). Thereafter, we have computed the fidelity of quantum state (ρ_{ideal} in Eq. (1)) and that obtained by the experiment performed using our optimized quantum circuit ($\rho_{ex}B$ in Eq. (4) and in Eq. (5)). For example, in case of Fig. 2 (a), we obtained the fidelity for the original circuit as 0.72, while that of our optimized circuit in Fig. 2 (b) is 0.90. Similarly, for Fig. 2 (c), we obtained the fidelity of the original circuit as 0.88, while that of our optimized circuit in Fig. 2 (d) is obtained to be 0.89. Thus, the optimization procedure clearly helps us in performing quantum computation with greater accuracy and to prepare the desired quantum states with higher fidelity.

4 More results: Optimized circuits for various quantum computing tasks

The algorithmic approach developed in [12] and followed here has been used to optimize various quantum circuits. They are summarized in Tables 3-5. Specifically, Tables 3 and 4 report results of circuit optimization algorithm applied on circuits for various quantum computing tasks using QX4 and QX2 processors, respectively. Interested readers may access the optimized circuits along with corresponding original circuits at <https://github.com/QBenchmark/benchmarks> [17]. From the Tables 3-5 and <https://github.com/QBenchmark/benchmarks> [17], it's clear that the optimization algorithm decreases gate counts and number of levels in most of the cases. In particular, we observe the best results of optimization of circuits for non-destructive discrimination of arbitrary set of orthogonal quantum states given in [18] for both QX4 and QX2 architectures (for details, see Tables 3 and 4: (67-78) % of reduction in gate counts and (57-63)% reduction in the levels are achieved for the circuits shown in Fig. (25-29) and in Fig. 1a of [18]). The optimization performances for various other circuits (see corresponding papers cited in the table) indexed in decreasing order are given. Table 5 contains optimization details of another set of circuits (which can be best described as reversible circuits) as given in [19]. Here we observe a maximum reduction of 72% in number of gates for circuit for evaluating the function **alu-v1_28** and 70% in the number of levels for circuit **alu-v4_37**. Clearly, the method used here can reduce the gate count and number of levels for most of the circuits implemented so far using IBM quantum processors. It can also efficiently optimize a large number of reversible circuits.

5 Conclusion

In this paper, we have shown that quantum circuits which have been designed until now, for the implementations in IBM quantum computers can be optimized in terms of gate count and the number of levels. It's further established that the reduction in these measures of circuit costs leads to improvement in the fidelity of the output state, and thus reduces the effect of noise or equivalently increases the accuracy of the quantum computation. As the effect of noise generally leads to an evolution of a quantum state towards a classical state, the reduction of noise through optimization of quantum circuits are expected to lead to clearer manifestation of quantum features. This has been clearly seen in the context of 3-qubit Mermin inequality, where the amount of violation of Mermin inequality can be quantified by $\langle M_3 \rangle - 2$, a greater value of which would correspond to the stronger signature of departure from the classical world. The optimized circuit has yielded a value of this quantity as 1.116 in contrast to the earlier reported value of 0.85, clearly indicating a stronger signature of non-locality. Thus, the optimized circuit illustrate the quantum feature in a more profound manner. Also, as expected the fidelity of the optimized circuits is found to be higher than their non-optimized counter parts. This establishes that to obtain best results using IBM quantum computers, one has to use our approach and keeping this fact in mind, we conclude this paper by noting that this work is expected to influence a large number of future works involving IBM quantum experience by providing a tool for obtaining best results. Of course, the results reported here are restricted to 5-qubit quantum computers, but the method used is general and the program can be scaled up for 16 qubit, 20 qubit and other bigger computers, too. The results for such systems will be reported elsewhere.

Ref	Fig	Initial		Final		% Reduction	
		Gates	Levels	Gates	Levels	Gates	Levels
[18]	26	18	8	4	3	78	63
[18]	27	19	9	5	4	74	56
[18]	29	19	8	5	4	74	50
[18]	25	17	8	5	4	71	50
[20]	1a	12	7	4	2	67	71
[18]	28	20	8	8	4	60	50
[7]	3	28	22	13	11	54	50
[21]	5	4	3	2	2	50	33
[22]	13a	8	6	4	3	50	50
[20]	1b	14	7	8	5	43	29
[21]	3	11	5	7	5	36	0
[6]	4b	11	7	7	5	36	29
[20]	2a	17	7	11	6	35	14
[21]	6	6	4	4	4	33	0
[23]	3	37	21	25	15	32	29
[21]	4	19	7	13	7	32	0
[24]	2	13	9	9	7	31	22
[20]	2b	20	7	14	8	30	-14
[6]	8	28	19	22	17	21	11
[22]	13b	10	6	8	5	20	17
[6]	3b	11	8	9	7	18	13
[25]	6	41	27	34	20	17	26
[26]	6	24	13	20	11	17	15
[27]	2	13	10	11	9	15	10
[26]	4	16	10	14	7	13	30
[27]	3	17	14	15	11	12	21
[28]	6	23	15	21	14	9	7
[23]	6	29	20	27	20	7	0
[29]	1	53	31	50	31	6	0
[30]	8	57	38	55	37	4	3

Table 3: Results of the optimization of the quantum circuits which were implemented earlier using IBM quantum processor. Here, the optimization is done using our algorithm and by considering the architecture used in QX4

Ref	Fig	Initial		Final		% Reduction	
		Gates	Levels	Gates	Levels	Gates	Levels
[18]	26	18	8	4	3	78	63
[18]	27	19	9	5	4	74	56
[18]	29	19	8	5	4	74	50
[18]	25	17	8	5	4	71	50
[20]	1a	12	7	4	2	67	71
[18]	28	20	8	8	4	60	50
[7]	3	28	22	13	11	54	50
[21]	5	4	3	2	2	50	33
[22]	13a	8	6	4	3	50	50
[23]	3	37	21	19	15	49	29
[20]	1b	14	7	8	5	43	29
[20]	2b	20	7	12	5	40	29
[21]	3	11	5	7	5	36	0
[6]	4b	11	7	7	6	36	14
[21]	6	6	4	4	4	33	0
[24]	2	13	9	9	7	31	22
[28]	6	23	15	17	11	26	27
[20]	2a	17	7	13	6	24	14
[22]	13b	10	6	8	5	20	17
[6]	3b	11	8	9	8	18	0
[25]	6	41	27	34	23	17	15
[27]	2	13	10	11	7	15	30
[27]	3	17	14	15	11	12	21
[30]	4	37	27	33	25	11	7
[30]	8	57	38	51	37	11	3
[30]	9	19	12	17	12	11	0
[26]	6	24	13	22	13	8	0
[30]	3	28	17	26	17	7	0
[6]	8	28	19	26	18	7	5
[23]	6	29	20	27	19	7	5
[30]	10	30	19	28	19	7	0
[29]	1	53	31	50	31	6	0

Table 4: Results of the optimization of the quantum circuits which were implemented earlier using IBM quantum processor. Here, the optimization is done using our algorithm and by considering the architecture used in QX2

Benchmarks	Initial	lines	Qiskit		RevKit		Improvements (%)	
			gates	levels	gates	levels	gates	levels
alu-v1_28	37	5	179	82	51	29	72	65
alu-v4_37	37	4	163	91	48	27	71	70
alu-v0_27	36	3	151	80	47	26	69	68
rd32-v1_68	36	3	123	70	41	27	67	61
alu-v2_33	37	3	144	79	50	27	65	66
alu-v1_29	37	3	138	73	48	26	65	64
a3x_c	48	3	143	71	52	39	64	45
rd32-v0_66	34	3	111	65	41	27	63	58
decod24-v0_38	51	5	180	99	67	42	63	58
mod5mils_65	35	5	140	79	54	35	61	56
one-two-three-v2_100	69	5	238	128	95	48	60	63
4gt11_82	27	5	136	69	55	33	60	52
alu-v0_26	84	5	295	157	120	72	59	54
a3x_d	44	5	116	69	48	33	59	52
one-two-three-v3_101	70	5	291	166	121	74	58	55
alu-v3_35	37	5	113	61	48	27	58	56
Full_Adder_c	20	5	58	38	25	22	57	42
mod5d1_63	22	5	90	49	39	27	57	45
mod5d2_64	53	5	206	119	94	61	54	49
4mod5-v1_22	21	5	74	40	35	23	53	43
decod24-v2_43	52	5	152	80	74	47	51	41
alu-v3_34	52	5	153	88	75	45	51	49
X1	51	5	127	64	63	30	50	53
decod24-v1_41	85	5	281	161	149	83	47	48
4mod5-v0_19	35	5	98	61	53	32	46	48
4mod5-v1_24	36	5	105	55	59	38	44	31
4mod5-v1_23	69	5	228	121	130	78	43	36
Full_Adder_e	21	5	58	30	34	18	41	40
a2x_c	31	5	67	40	40	28	40	30
decod24-v3_45	150	4	462	275	281	179	39	35
17	43	4	149	91	91	55	39	40
4gt5_76	91	5	294	146	182	111	38	24
a2x_e	30	5	66	38	41	27	38	29
alu-v4_36	115	5	339	185	211	123	38	34
hwb4_49	233	5	788	430	494	315	37	27
4gt13_90	107	5	309	163	200	116	35	29
aj-e11_165	151	5	448	242	294	182	34	25
4_49_16	217	5	633	332	418	262	34	21
7	60	5	165	97	111	65	33	33
4mod5-v0_20	20	5	46	26	31	20	33	23
rd32_270	84	5	216	114	155	98	28	14
alu-v2_32	163	5	423	221	309	175	27	21
4gt11_84	18	5	34	20	25	12	26	40
4mod7-v0_94	162	5	399	230	299	184	25	20
Full_Adder_d	22	5	49	32	37	24	24	25
4mod5-v0_18	69	4	173	102	139	91	20	11
alu-v2_31	451	5	1163	625	942	578	19	8
mini-alu_167	288	4	712	369	577	353	19	4
4gt10-v1_81	148	5	348	183	286	174	18	5
Toffoli_e	17	3	23	14	19	12	17	14
4gt13-v1_93	68	4	104	51	86	48	17	6
4gt13_91	103	4	227	131	199	111	12	15
ex-1_166	19	4	26	18	23	15	12	17

Table 5: Results of the optimization of the reversible circuits. The optimization is done using our algorithm and by considering the architecture used in QX4. Here, initial circuits correspond to the Clifford+T circuits for various functions available in [17]. No restriction on application of CNOT gates is applied in the initial circuits. Considering the restrictions on CNOT gates implied by the architecture of QX4, the columns under Qiskit [31] is obtained. Finally, those same circuits are optimized using our algorithm and the corresponding results are shown in the columns under RevKit [32], as the RevKit platform is used by us.

Acknowledgments

A.S. gratefully acknowledge University of Science and Technology of China (USTC), Hefei, P. R. C. for providing support. A.A.A. is grateful for the support of Coordenação de Aperfeiçoamento de Pessoal de Nível Superior - Brasil (CAPES) - Finance Code 001, and he also thanks Universidade Estadual Paulista (UNESP), Faculdade de Engenharia de Ilha Solteira, Câmpus de Ilha Solteira. G.W.D. and A.A.A. also acknowledge the support of the Natural Sciences and Engineering Research Council of Canada (NSERC). A.P. thanks the Department of Science and Technology (DST), India, for support provided through the DST project No. EMR/2015/000393.

References

- [1] Grover, L. K.: Quantum mechanics helps in searching for a needle in a haystack. *Physical Review Letters* **79**, 325 (1997)
- [2] Shor, P. W.: Polynomial-time algorithms for prime factorization and discrete logarithms on a quantum computer. *SIAM review* **41**, 303–332 (1999)
- [3] Bennett, C. H., Brassard, G., Crépeau, C., et al.: Teleporting an unknown quantum state via dual classical and Einstein-Podolsky-Rosen channels. *Physical Review Letters* **70**, 1895 (1993)
- [4] Shenoy-Hejamadi, A., Pathak, A., Radhakrishna, S.: Quantum cryptography: Key distribution and beyond. *Quanta* **6** (2017)
- [5] IBM Q. <https://www.research.ibm.com/ibm-q/>. Accessed: 2018-11-05
- [6] Sisodia, M., Shukla, A., Pathak, A.: Experimental realization of nondestructive discrimination of Bell states using a five-qubit quantum computer. *Physics Letters A* **381**, 3860–3874 (2017)
- [7] Sisodia, M., Shukla, A., Thapliyal, K., Pathak, A.: Design and experimental realization of an optimal scheme for teleportation of an n-qubit quantum state. *Quantum Information Processing* **16**, 292 (2017)
- [8] Yalçınkaya, İ., Gedik, Z.: Optimization and experimental realization of the quantum permutation algorithm. *Physical Review A* **96**, 062339 (2017)
- [9] Behera, B. K., Banerjee, A., Panigrahi, P. K.: Experimental realization of quantum cheque using a five-qubit quantum computer. *Quantum Information Processing* **16**, 312 (2017)
- [10] Alsina, D., Latorre, J. I.: Experimental test of Mermin inequalities on a five-qubit quantum computer. *Physical Review A* **94**, 012314 (2016)
- [11] Shukla, A., Sisodia, M., Pathak, A.: Complete characterization of the single-qubit quantum gates used in the IBM quantum processors. *arXiv preprint arXiv:1805.07185* (2018)
- [12] Dueck, G. W., Pathak, A., Rahman, M. M., Shukla, A., Banerjee, A.: Optimization of circuits for IBM’s five-qubit quantum computers. in: 2018 21st Euromicro Conference on Digital System Design (DSD) pp. 680–684 IEEE (2018)
- [13] IBM Q5 Yorktown. <https://github.com/Qiskit/ibmq-device-information/tree/master/backends/yorktown/V1>. Accessed: 2018-11-05
- [14] IBM Q5 Tenerife. <https://github.com/Qiskit/ibmq-device-information/tree/master/backends/tenerife/V1>. Accessed: 2018-11-05
- [15] Lanyon, B., Zwerger, M., Jurcevic, P., et al.: Experimental violation of multipartite Bell inequalities with trapped ions. *Physical Review Letters* **112**, 100403 (2014)
- [16] Zhao, Z., Yang, T., Chen, Y.-A., et al.: Experimental violation of local realism by four-photon Greenberger-Horne-Zeilinger entanglement. *Physical Review Letters* **91**, 180401 (2003)

- [17] Reversible and Quantum Benchmark Circuits. <https://github.com/QBenchmark/benchmarks>
- [18] Majumder, A., Kumar, A.: Experimental demonstration of non-destructive discrimination of arbitrary set of orthogonal quantum states using 5-qubit ibm quantum computer on cloud. arXiv preprint arXiv:1803.06311 (2018)
- [19] Große, D., Wille, R., Dueck, G. W., Drechsler, R.: Exact synthesis of elementary quantum gate circuits for reversible functions with don't cares. in: Int'l Symp. on Multi-Valued Logic pp. 214–219 (2008)
- [20] Alsina, D., Latorre, J. I.: Experimental test of Mermin inequalities on a five-qubit quantum computer. *Physical Review A* **94**, 012314 (2016)
- [21] Deffner, S.: Demonstration of entanglement assisted invariance on ibm's quantum experience. *Heliyon* **3**, e00444 (2017)
- [22] García-Martín, D., Sierra, G.: Five experimental tests on the 5-qubit IBM quantum computer. *Journal of Applied Mathematics and Physics* (2018)
- [23] Behera, B. K., Seth, S., Das, A., Panigrahi, P. K.: Demonstration of entanglement purification and swapping protocol to design quantum repeater in IBM quantum computer. arXiv preprint arXiv:1712.00854v2 (2018)
- [24] Srinivasan, K., Behera, B. K., Panigrahi, P. K.: Solving linear systems of equations by gaussian elimination method using grover's search algorithm: An IBM quantum experience. arXiv preprint arXiv:1801.00778 (2017)
- [25] Li, R., Alvarez-Rodriguez, U., Lamata, L., Solano, E.: Approximate quantum adders with genetic algorithms: an IBM quantum experience. *Quantum Measurements and Quantum Metrology* **4**, 1–7 (2017)
- [26] Vishnu, P., Joy, D., Behera, B. K., Panigrahi, P. K.: Experimental demonstration of non-local controlled-unitary quantum gates using a five-qubit quantum computer. *Quantum Information Processing* **17**, 274 (2018)
- [27] Kalra, A. R., Prakash, S., Behera, B. K., Panigrahi, P. K.: Demonstration of the quantum no-hiding theorem in a category theoretic framework: An IBM quantum experience (2017)
- [28] Satyajit, S., Srinivasan, K., Behera, B. K., Panigrahi, P. K.: Nondestructive discrimination of a new family of highly entangled states in IBM quantum computer. *Quantum Information Processing* **17**, 212 (2018)
- [29] Gurnani, K., Behera, B. K., Panigrahi, P. K.: Demonstration of optimal fixed-point quantum search algorithm in IBM quantum computer. arXiv preprint arXiv:1712.10231v1 (2017)
- [30] Ghosh, D., Agarwal, P., Pandey, P., Behera, B. K., Panigrahi, P. K.: Automated error correction in IBM quantum computer and explicit generalization. *Quantum Information Processing* **17**, 153 (2018)
- [31] Qiskit - An open-source framework for working with noisy intermediate-scale quantum computers (NISQ) at the level of pulses, circuits, and algorithms. <https://github.com/Qiskit>
- [32] Soeken, M., Frehse, S., Wille, R., Drechsler, R.: RevKit: a toolkit for reversible circuit design. in: *Proceedings of the International Symposium on Multiple-Valued Logic* (2008). RevKit is available at <https://github.com/msoeken/cirkit>